PHASE-STRUCTURAL COMPOSITION OF COATING OBTAINED BY PULSED PLASMA TREATMENT USING ERODED CATHODE OF T1 HIGH SPEED STEEL

Yu.G. Chabak[1], V.I. Fedun[1], K. Shimizu[2], V.G. Efremenko[1], V.I. Zurnadzhy[1]
[1]Priazovskyi State Technical University, Mariupol, Ukraine;
[2]Muroran Institute of Technology, Muroran-city, Hokkaido, Japan
E-mail: julia.chabak@yandex.ua, vgefremenko@gmail.com

The structure and distribution of chemical elements in the coating obtained in the high-chromium cast iron by plasma treatment with a high-current pulsed electric discharge using a cathode made of T1 high speed steel (18%W) are investigated. It is found that the plasma treatment followed by quenching result in formation of modified layer and hard coating with large amount of tungsten carbides. The data on the structural and phase composition, micro-hardness and distribution of chemical elements in the cross section of the modified layer and coating are presented.

PACS: 52.77. - j

INTRODUCTION

Pulsed plasma treatment (PPT) is becoming widely used for the surface hardening of machine parts and tools [1–3]. There are numerous works by Yu. Tyurin, A. Pogrebnyak et al., dedicated to the technology of modifying and protective coating deposition based on PPP with electric current switching by ionised products of explosion [4–6]. An alternative method of generating the plasma pulse is a high current electrical discharge in the chamber of axial electro-thermal axial plasma accelerator (ETPA). The construction and operational physical aspects of ETPA are described in detail by Yu. Kolyada et al. in works [7–9], where the great opportunities of this method for scientific and industrial applications are shown. Plasma treatment with the use of ETPA allows to modify the treated surface due to high-speed heating/quenching followed by formation of fine crystalline martensite [10, 11]. Besides, EPTA allows to combine the surface modification with deposition of protective coatings [6]. Formation of coating occurs due to sedimentation of atoms, ions, microdroplets which are transported by plasma flux from the cathode after its erosion induced by electric discharge. The above-mentioned papers are focused on the selection of optimal operating parameters of ETPA for nanopowders fabrication and surface hardening of low-alloyed steels. However, they do not concern the effect of cathode material on the structure and properties of the coatings. The cathode material usually used for plasma treatment is tungsten [10] or low-carbon steel [8, 9].

High-carbon iron-based alloys have been traditionally used as materials for wear applications. These alloys include white cast irons alloyed with carbide-forming elements (Cr, V, W, Ti, Nb etc.) [11–13]. Cast irons contain in the structure a substantial (tens of percent) volume fraction of very hard phases (carbides, carbonitrides, borides etc.), that makes them be wear resistant under abrasion, erosion etc. Typically the white alloyed cast irons are subjected to bulk heat treatment which improves their wear performance due to phase-structural transformations [14, 15]. Up to now, the plasma surface treatment of alloyed cast irons still remains substantially unstudied. In the present work the pulsed plasma technique was for the first time performed for strengthening high-chromium cast iron. Herewith, a new type of cathode, made of highly wear-resistant material, was used for the first time as well. The objective of this work was to study the structure and properties of modified layer and the coating formed on the surface of 15%Cr-cast iron by using the PPT with cathode made of T1 high speed steel.

1. EXPERIMENTAL

The substrate material was cast iron of the chemical composition: 2.70% Cr; 1.32% Si; 3.96% Mn; 0.21% Ni; 0.04% V; 0.10% Ti. The samples of 10x10x25 mm size were cut out of sand-mold casting and then subsequently annealed at 650 ^{o}C to produce a microstructure consisting of pearlite matrix and eutectic chromium carbides M_7C_3.

PPT of the samples was performed using the electro-thermal plasma accelerator. ETPA design, circuitry and principle of operation are described in [7–9]. PPT was carried out as follows: the voltage of the charge of capacitive energy storage device (1.5 mF) is 4 kV; the distance between the electrodes is 50 mm; current pulse shape is bell-like; the current amplitude is about 10 kA. As the discharge chamber tubular arrester RTF-6-0,5/10 U1 was used; a central electrode (cathode) was a rod 5 mm with diameter made of T1 high speed steel (0.75% C; 17.92% W; 3.85% Cr; 0.34% Mn; 0.30% Si; 1.07% V). The distance from the edge of ETPA to the target surface was 50 mm. The treatment was performed in an air environment, exposing tenfold plasma impulses. After PPT the samples were subjected to heat treatment consisted of heating at 950 °C with holding duration of 2 hours followed by oil quenching.

The microstructure was examined in cross section of the microprobes prepared according to the standard procedure and etched with 4%-nital solution. The optical microscope Nikon Eclipse M200 and scanning electron microscope JEOL JSM-6510 LV were employed for the microstructure analyzing. The volume fraction (VF) of carbides was calculated manually on SEM micrographs using known Rosiwal's lineal analysis. The phase elements distribution and chemical composition was investigated by using an energy-dispersive spectroscopy (EDS) with the detector X-Act detector (Oxford Instruments). The phase composition of the coating was determined by X-ray diffractometer DRON-3 in K_α

radiation. Microhardness was measured using FM-300 (Future-Tech) tester under a load of 50 g.

2. THE RESULTS AND DISCUSSION

The microstructural studies have shown that PPT and quenching resulted in formation of the coating on the cast iron surface (Fig. 1). The coating thickness is 160…170 μm; it is characterized by large number of white inclusions lying against the dark background. The volume fraction and the dispersity of inclusions varied with depth non-monotonically, indicating coating structure lamination (Fig. 2,a). It should be noted that the correlation between the size of the carbides and their volume fraction was not observed.

The inclusions VF values were found to be in the range of 31…61%. The minimum inclusions VF corresponded to their maximum size (average diameter 3.0…3.6 μm) in outer layer at a depth of 25…40 μm. The most disperse inclusions were detected in the intermediate layer of 15…20 μm thickness lying between the coating and the substrate in a layer; in this layer the average size and the VF of the inclusions were measured as 1.0 μm and 32% respectively.

According to Fig. 2,b, the coating is distinguished by high microhardness. At the very surface the microhardness value is 1230…1270 HV_{50}. At a depth of 30…70 μm the microhardness values decreases to 1070…1220 HV_{50} and further increases to 1200…1325 HV_{50} at a depth of 90…120 μm. Close to the border with the substrate the microhardness is reduced to 1110…1260 HV_{50}, All these values are higher as compared to substrate microhardness (930…1070 HV_{50}). Analysis of the data given in Fig. 2, showed that the lowest microhardness values are attributed to the layer with the coarsest inclusions at their minimum volume fraction.

XRD phase identification revealed the presence of αFe-based and γFe-based solid solutions in the coating (Fig. 3). Considering the fact that the coating was heat treated, these solid solutions were identified as martensite and retained austenite. According to the ratio of peaks $(110)_{\alpha Fe}$ and $(111)_{\gamma Fe}$ intensities, the metallic matrix in coating is mostly martensite. Besides, the XRD-pattern contains the numerous diffraction peaks attributed to carbide phases (Table). Some of these peaks correspond to the interplanar distance, which can be referred to different carbides, making phase identification difficult. Only using the authentic peaks the presence of carbides M_6C, M_2C, MC, M_3C was clearly proved. Based on peaks intensity, it can be assumed that W-based carbide M_6C is dominant among the carbide phases; the volume fractions of MC carbide and alloyed cementite M_3C are minimum. Since the coating was deposited using the cathode of T1 steel, thus it was concluded that the inclusions found in the coating structure are mainly W-rich carbides $(W_3Fe_3)C$ [16].

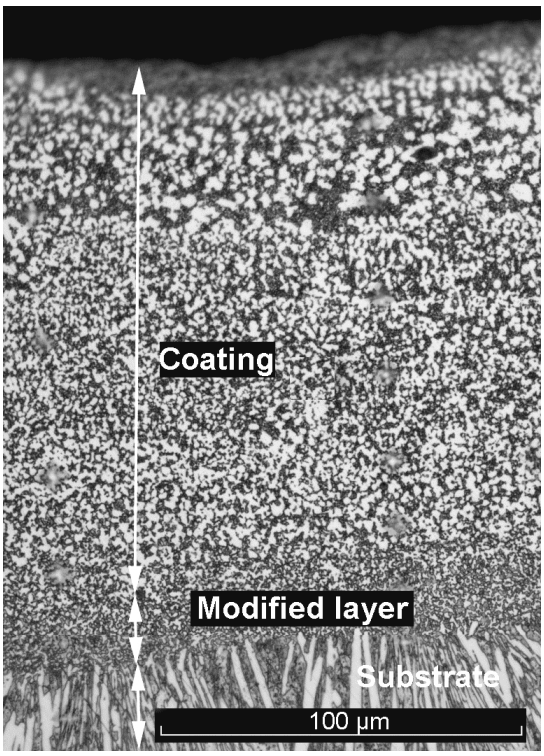

Fig. 1. The microstructure of plasma coating

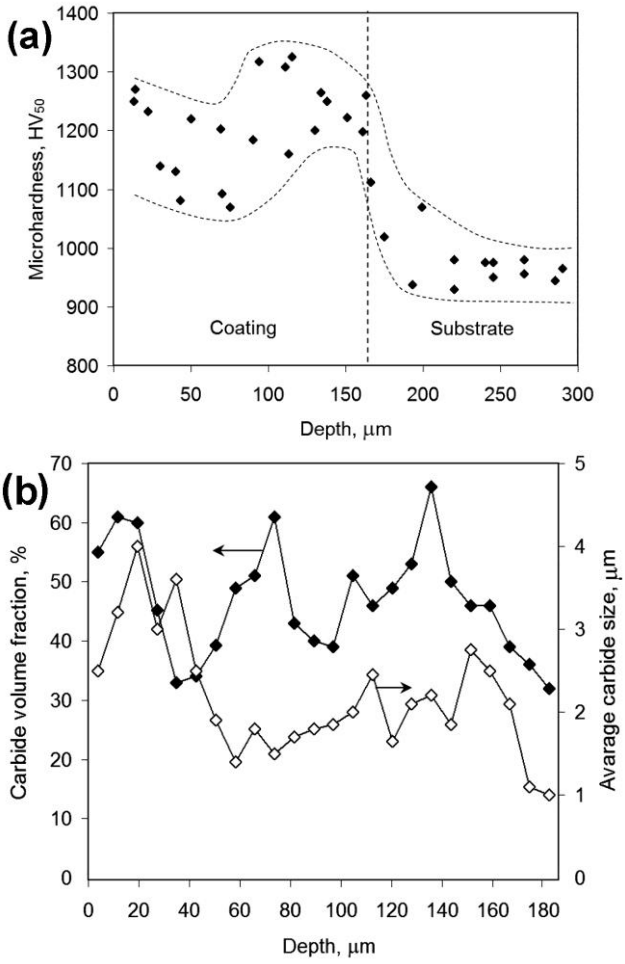

Fig. 2. The microhardness (a) and inclusions VF size (b) as a function of layer depth

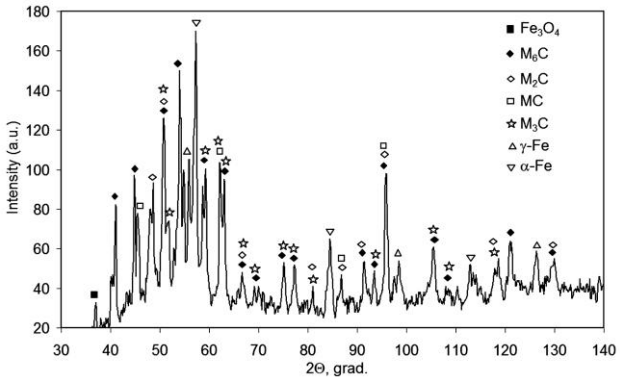

Fig. 3. XRD-pattern of coating

Carbide phases reflexes

2Θ, grad	d/n	Phases (hkl)
40.8	2.778	Me_6C (400)
44.6	2.550	Me_6C (331)
45.7	2.498	MeC (100)
48.6	2.352	Me_2C (002)
50.8	2.258	Me_2C (111), M_6C (111), M_3C (111)
51.8	2.217	M_3C (200)
54.0	2.135	Me_6C (511)
59.1	1.963	M_6C (440), M_3C (211)
62.1	1.877	MC (101), M_3C (113)
63.3	1.846	M_6C (442), M_3C (122)
66.7	1.763	M_6C (620), Me_2C (102), M_3C (212)
69.2	1.707	M_6C (622), M_3C (023)
75.5	1.583	M_2C (003), M_3C (130)
77.3	1.551	M_6C (551), M_3C (311)
81.7	1.482	M_2C (110), M_3C (222)
86.8	1.410	MC (002), M_2C (111)
91.5	1.353	M_6C (733), M_2C (103)
93.5	1.330	M_6C (644), M_3C (230)
95.7	1.307	M_6C (822), Me_2C (200), MC (111)
105.5	1.217	M_6C (733), M_3C (322)
108.5	1.194	M_6C (664), M_3C (025)
118.5	1.127	M_2C (202), M_3C (330)
121.0	1.113	M_6C (933)
129.7	1.070	M_6C (773), M_2C (104)

XRD measurements were supported by EDS-study of phase elemental distribution (Fig. 4). Fig. 4a presents the secondary electron image (SEI-mode) of coating microstructure. As can be seen, carbides M_6C are the coarse inclusions joined in thick continuous network lying along the grain boundaries. According to Fig 4b-d («mapping»-mode) carbides M_6C are enriched with tungsten and chromium but depleted in iron. The matrix plots adjacent to the carbides were found to have an increased Cr and W concentration. On the contrary, matrix areas lying in the distance from carbides are enriched with iron. EDS-point analyzing showed that M_6C contained 6.99% C, 6.17% Cr, 70.57% Fe, 14.93% W (Fig. 5,a).

Beside M_6C carbides, the structure contains small granular inclusions, which are distinguished in Fig. 4,a as bright white dots, located inside matrix grains and along the coarse carbides boundaries. According to Fig. 4,b, the small inclusions are enriched with tungsten and depleted in chromium as compared to M_6C carbides. EDS-point results for granular inclusions are: 7.32% C, 1.82% Cr, 66.09% Fe, 22.32% W (see Fig. 5,b)). This indicates that granular inclusions are W-rich carbides M_2C [16].

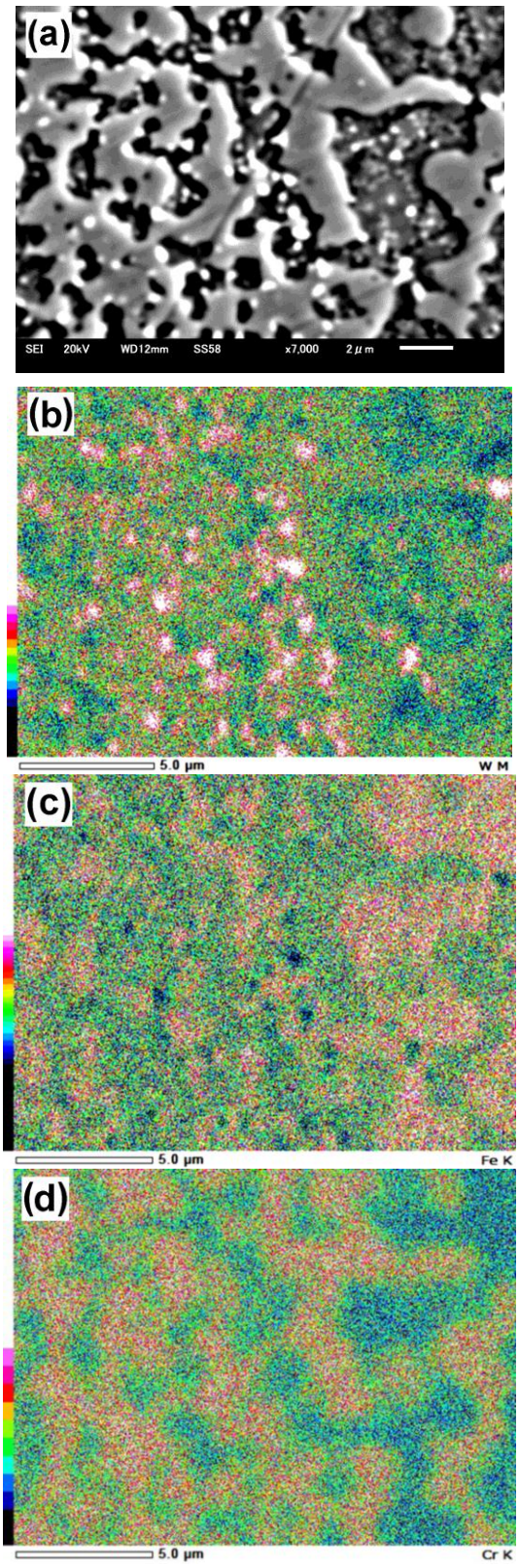

Puc. 4. SEI-image of coating microstructure (a) and the distribution of W (b); Fe (c), and Cr (d) within the same area

EDS-point results for tungsten content in M_6C and M_2C carbides turned out to be two times smaller than it had been expected [16]. It should be admitted that the quantitative EDS method did not exactly characterize the chemical composition of the carbides because of their small size, in connection with which the results obtained could be greatly affected by surrounding matrix areas.

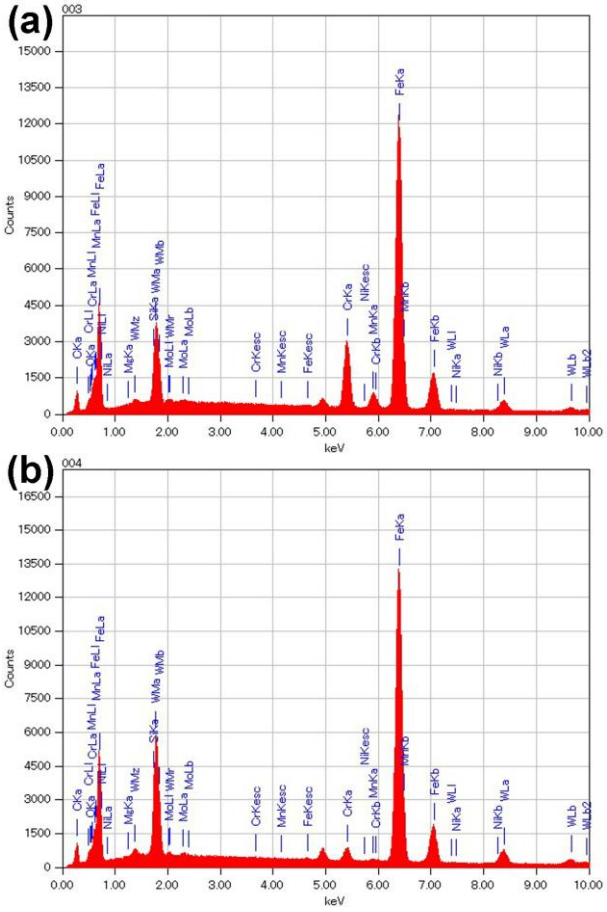

Fig. 5. EDS-spectra of carbides M_6C (a) and M_2C (b)

Electron probe micro-analysis showed inhomogeneous distribution of tungsten and chromium within the coating. Fig. 6 shows the coating area adjacent to the substrate metal. The images are given in SEI-mode (a) and back-scattered electrons (BEC-mode) (b). The latter mode allows to detect the distribution of elements differing in atomic number: the areas enriched with heavy elements (with higher Z) are lighter in color and vice versa. A comparison of SEI- and BEC-images shows that the coating plot with coarse carbides M_6C has a lighter colorization, i.e. it is enriched with a heavier element (tungsten). An increased amount of this element is detected in M_6C carbides and especially - in granular carbides of M_2C (see Fig. 6,b). The transition layer adjacent to the substrate is characterized by a darker colorization, indicating either absence or lower content of tungsten. The carbides in transition layer have a lighter color as compared to the large eutectic carbide in the substrate. The latter indicates that these carbides are enriched with iron and depleted in chromium unlike the eutectic carbides. The absence of tungsten and lower chromium content in carbides in transition layer are also confirmed by EDS line-scan mode reflecting the elemental distribution along the line shown in Fig. 7.

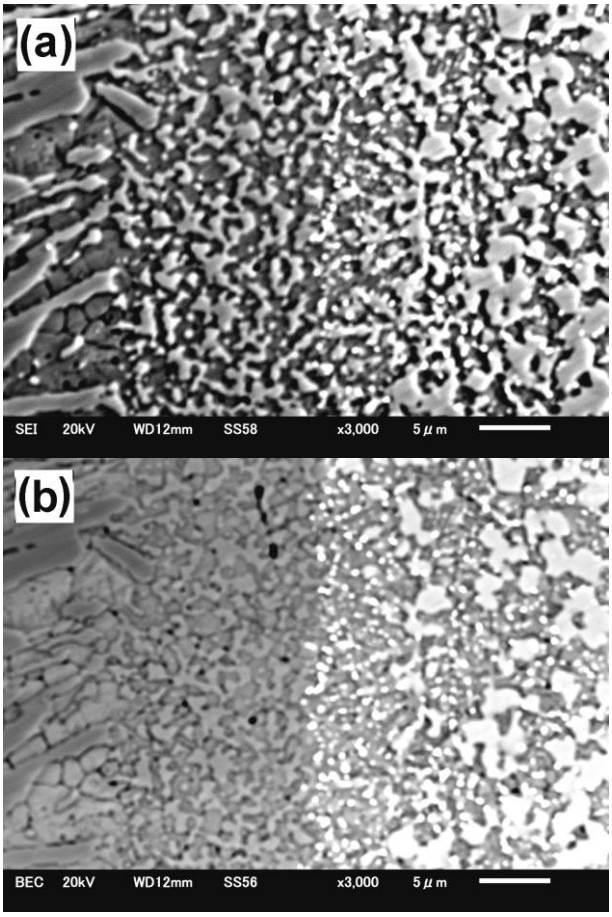

Fig. 6. The microstructure of transition zone: SEI-image (a), BEC-image (b)

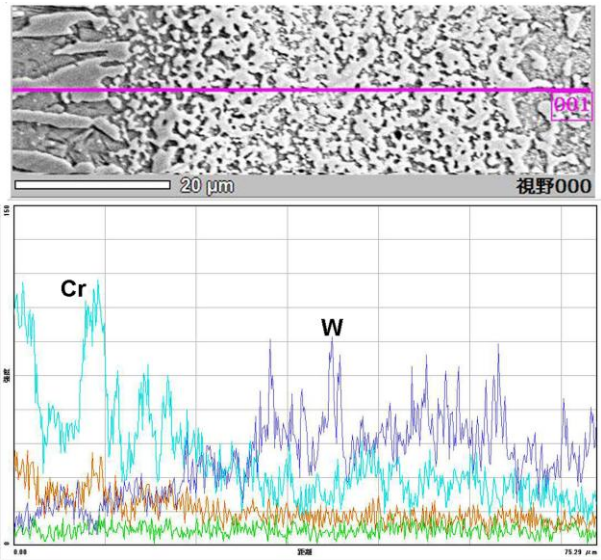

Fig. 7. The chemical elements distribution in transition layer

A study of chemical elements distribution allowed to assume that transition layer is the substrate surface layer thermally modified by plasma flux. It is very likely that it was formed as a result of substrate surface melting under plasma heating. The melting was facilitated by lower solidus temperature of cast iron due to presence of the fusible carbide eutectic. When melting the eutec-

tic carbides dissolved led to saturation of liquid with chromium. When solidifying, the supersaturated solid solution of chromium formed on the surface. Further, it decomposed with carbides precipitation during heat treatment. The size of carbides precipitates is much lower as compared to eutectic carbides; besides, they have lower chromium content that reflects their metastable nature. The transition layer is harder then substrate, thus it is modified by plasma treatment. It should be noted that there is no clearly defined boundary between the transition layer and the coating. It means that the formation of modified layer occurs almost simultaneously with cathode material crystallization. It was actually resulted in production of durable weld zone between the coating and the modified layer. Thus, the latter could be considered as an underlayer, which strongly bonds the coating and the substrate.

XRD showed that the coating contains W-rich carbide phases – a stable carbide M_6C, MC and metastable carbide M_2C. During solidification the latter partially transforms at elevated temperature into M_6C and MC according to the reaction $M_2C+\gamma Fe \rightarrow M_6C + MC$ [16]. Assuming the ultra fast crystallization of cathode material molten drops, then a supersaturated solid solution of the components (C, W, Cr, V) can be expected [17]. A great number of W-rich carbides precipitated out of this solution at quenching heating. A similar phenomenon is observed in the high chromium cast iron when primary austenite decomposes at high temperatures (destabilization process) [18]. However, if the secondary Cr-rich carbides precipitate as nanosized isolated inclusions [19], then in plasma coating the coarse W-rich carbides were found to be formed as continuous network. It is obvious, that carbides nature is largely affected by solid solution substructure and its saturation with tungsten and carbon.

The coating structure differs from the cathode material with significantly higher volume fraction of carbide phases. It is known that the numbers of carbides in high-speed steels do not exceed 20% [20]; on the contrary, in the plasma coating the carbides VF reached 61%. One can assume that in the course of the PPT the cathode material had been enriched with carbon that further caused the increase in the carbides VF. Indeed, the evaporation of paper-bakelite of ETPA inner chamber and dissipation during the discharge could lead to involving carbon particles into plasma. Getting on the surface of microdroplets and liquid substrate the carbon enriched the melt.

Thus, the investigations have shown that PPT can be successfully applied for surface strengthening of high chromium cast iron. The usage of the electro-plasma accelerator allows to provide the surface modification with simultaneous protective coating deposition. In this process, the cathode material plays a key role defining the coating structure. In order to obtain a wear-resistant coating the cathode should contain an increased amount of carbide-forming elements. In study case high tungsten tool steel has been used, although other options are possible, for example, white cast iron, sintered materials, composites, etc. The selection of optimal cathode material for the manufacturing wear resistant coatings is of interest for further research.

CONCLUSIONS

1. For the first time pulsed plasma treatment using electro-thermal axial plasma accelerator was applied for 15% Cr white cast iron. After ten pulses the surface modified layer of 15…20 μm thick and the coating of 150 μm thick were obtained.

2. PPT and subsequent quenching resulted in formation of the coating consisting of martensite-austenite matrix and 31…61% of W-rich carbides M_6C, M_2C and MC. The microhardness values were achieved as follows: in modified layer – 1110…1260 HV_{50}, in the coating – 1070…1325 HV_{50}, in the substrate – 930…1070 HV_{50}.

3. Pulsed plasma treatment using ETPA is accompanied with carbon enrichment of melt which results in carbides VF increasing relatively cathode material.

REFERENCES

1. S. Romankov, A. Mamaeva, S.D. Kaloshkin, S.V. Komarov. Pulsed plasma treatment of Ti-Al coatings produced by mechanical alloying method // *Materials Letters*. 2007, v. 26, issue 30, p. 5288-5291.

2. Y.Y. Özbek, H. Akbulut, M. Durman. Surface behavior of AISI 4140 modified with the pulsed-plasma technique // *Materials and Technology*. 2015, v. 49, issue 3, p. 441-445.

3. N. Espallargas, S. Mischler. Dry wear and tribocorrosion mechanisms of pulse plasma nitrided Ni-Cr alloy // *Wear*. 2011, v. 270, issue 7-8, p. 464-471.

4. M. Kovaleva, Yu. Tyurin, N. Vasilik, O. Kolisnichenko, M. Prozorova, M. Arseenko, E. Danshina. Deposition and characterization of Al_2O_3 coatings by multi-chamber gas-dynamic accelerator // *Surface and Coatings Technology*. 2013, v. 232, p. 719-725.

5. N.J. Vasilik, Y.N. Tyurin, O.V. Kolisnichenko, M.G. Kovaleva, M.S. Prozorova, M.Y. Arseenko. Properties, peculiarities and applications of powder coatings formed by multi-chamber detonation sprayer // *Applied Mechanics and Materials.* 2014, v. 467, p. 179-184.

6. А.Д. Погребняк, Ю.Н. Тюрин. Импульсно-плазменная модификация свойств поверхности и нанесение покрытий // *Успехи физики металлов*. 2003, т. 4, с. 1-66.

7. Yu.E. Kolyada, V.I. Fedun, V.I. Tyutyunnikov, N.A. Savinkov, A.E. Kapustin. Formation mechanism of the metallic nanostructures using pulsed axial electrothermal plasma accelerator // *Problems of Atomic Science and Technology. Series "Plasma Electronics and New Acceleration Methods"*. 2013, N 4(86), p. 297-300.

8. Yu.E. Kolyada, V.I. Fedun. Pulse electrothermal plasma accelerators and its application in scientific researches // *Problems of Atomic Science and Technology. Series "Plasma Electronics and New Acceleration Methods"*. 2015, N 4, p. 325-330.

9. Yu.E. Kolyada, A.A. Bizyukov, O.N. Bulanchuk, V.I. Fedun. Pulse electrothermal plasma accelerators and its application in the technologies // *Problems of Atomic Science and Technology. Series "Plasma Electronics and New Acceleration Methods"*. 2015, N 4, p. 319-324.

10. S.S. Samotugin, V.I. Lavrinenko, E.V. Kudinova, Yu.S. Samotugina. The influence of plasma surface modification process on the structure and phase composition of cutting-tool hardmetals // *Journal of Superhard Materials.* 2011, N 3 (33), p. 200-207.

11. V.G. Efremenko, K. Shimizu, A.P. Cheiliakh, T.V. Kozarevs'ka, Yu.G. Chabak, H. Hara, K. Kusumoto. Abrasive wear resistance of spheroidal vanadium carbide cast irons // *Journal of Friction and Wear*. 2013, issue 34, p. 466-474.

12. H. Gasan, F. Erturk. Effects of a destabilization heat treatment on the microstructure and abrasive wear behavior of high-chromium white cast iron investigated using different characterization techniques // *Metallurgical and Materials Transactions A.* 2013, v. 44, issue 11, p. 4993-5005.

13. V.G. Efremenko, K. Shimizu, A.P. Cheiliakh, T.V. Kozarevskaya, K. Kusumoto, and K.Yamamoto. Effect of vanadium and chromium on the microstructural features of V-Cr-Mn-Ni spheroidal carbide cast irons // *International Journal of Minerals, Metallurgy and Materials*. 2014, v. 21, p. 1096-1108.

14. A. Bedolla-Jacuinde, F.V. Guerra, I. Mejía, J. Zuno-Silva, M. Rainforth. Abrasive wear of V-Nb-Ti alloyed high-chromium white irons // *Wear*. 2015, v. 332-333, p. 1006-1011.

15. V.G. Efremenko, Yu.G. Chabak, M.N. Brykov. Kinetic parameters of secondary carbide precipitation in high-Cr white iron alloyed by Mn-Ni-Mo-V complex // *Journal of Materials Engineering and Performance*. 2013, v. 22, p. 1378-1385.

16. A.S. Chaus. Microstructural and properties evaluation of M2 high speed steel after inoculating addition of powder W and WC // *Materials Science and Technology*. 2014, v. 30, N 9, p. 1105-1115.

17. Y.Y. Özbek, H. Akbulut, M. Durman. Surface properties of M2 steel treated by pulse plasma technique // *Vacuum*. 2015, v. 122, part A, p. 90-95.

18. V. Efremenko, K. Shimizu, Yu. Chabak. Effect of destabilizing heat treatment on solid-state phase transformation in high-chromium cast irons // *Metallurgical and Materials Transactions A.* 2013, v. 44, issue 12, p. 5434-5446.

19. Yu.G. Chabak, V.G. Efremenko. Change of secondary-carbides' nanostate in 14.5% Cr cast iron at high-temperature heating // *Metallofizika i Noveishie Tekhnologii.* 2012, v. 34, N 9, p. 1205-1220 (in Russian).

20. R.A. Nogueira, O.C.S. Ribeiro, M.D.M. Neves, L. Salgado, F.F. Ambrozio. Effect of heat treatment on microstructure of commercial and vacuum sintered high speed steels AISI M2 and T15 // *Materials Science Forum.* 2005, v. 498-499, p. 186-191.

Article received 21.03.2016

ФАЗОВО-СТРУКТУРНЫЙ СОСТАВ И СВОЙСТВА ПОКРЫТИЯ, ПОЛУЧЕННОГО ИМПУЛЬСНО-ПЛАЗМЕННОЙ ОБРАБОТКОЙ С ИСПОЛЬЗОВАНИЕМ ЭРОДИРУЮЩЕГО КАТОДА ИЗ СТАЛИ Р18

Ю.Г. Чабак, В.И. Федун, К. Шимидзу, В.Г. Ефременко, В.И. Зурнаджи

Исследовано строение и распределение химических элементов в покрытии, полученном на высокохромистом чугуне плазменной обработкой с применением сильноточного импульсного электрического разряда при использовании катода из стали Р18. Установлено, что в результате обработки образуются имеющие высокую твердость модифицированный слой и покрытие, содержащее большое количество карбидов вольфрама. Приведены данные о структурном и фазовом составе, микротвердости и распределению химических элементов по сечению модифицированного слоя и покрытия.

ФАЗОВО-СТРУКТУРНИЙ СКЛАД І ВЛАСТИВОСТІ ПОКРИТТЯ, ОТРИМАНОГО ІМПУЛЬСНО-ПЛАЗМОВОГО ОБРОБКОЮ З ВИКОРИСТАННЯМ КАТОДА ЗІ СТАЛІ Р18, ЩО ЕРОДУЄ

Ю.Г. Чабак, В.І. Федун, К. Шимідзу, В.Г. Єфременко, В.І. Зурнаджи

Досліджено будову і розподіл хімічних елементів в покритті, отриманому на високохромистого чавуну плазмовою обробкою із застосуванням потужнострумового імпульсного електричного розряду при використанні катода зі сталі Р18. Встановлено, що в результаті обробки формується модифікований шар чавуну і покриття, яке містить велику кількість карбідів вольфраму і має високу твердість. Наведено дані про структурний і фазовий склад, мікротвердості і розподілу хімічних елементів по перерізу модифікованого шару і покриття.